ARTHRITIS & RHEUMATOLOGY
Vol. 66, No. 8, August 2014, pp 2047–2058
DOI 10.1002/art.38648

Fucosyltransferase 1 Mediates Angiogenesis in Rheumatoid Arthritis

Takeo Isozaki,[1] Mohammad A. Amin,[1] Jeffrey H. Ruth,[1] Phillip L. Campbell,[1] Pei-Suen Tsou,[1] Christine M. Ha,[1] W. Alex Stinson,[1] Steven E. Domino,[1] and Alisa E. Koch[2]

Objective. **To determine the role of α(1,2)-linked fucosylation of proteins by fucosyltransferase 1 (FUT1) in rheumatoid arthritis (RA) angiogenesis.**

Methods. **Analysis of α(1,2)-linked fucosylated proteins in synovial tissue (ST) samples was performed by immunohistologic staining. Expression of α(1,2)-linked fucosylated angiogenic chemokine in synovial fluid (SF) was determined by immunoprecipitation and lectin blotting. To determine the angiogenic role of α(1,2)-linked fucosylated proteins in RA, we performed human dermal microvascular endothelial cell (HMVEC) chemotaxis and Matrigel assays using sham-depleted and α(1,2)-linked fucosylated protein–depleted RA SF samples. To examine the production of proangiogenic chemokines by FUT1 in HMVECs, cells were transfected with FUT1 sense or antisense oligonucleotides, and enzyme-linked immunosorbent assay was performed. We then studied mouse lung endothelial cell (EC) chemotaxis using wild-type and FUT1 gene–deficient mouse lung ECs.**

Results. **RA ST endothelial cells showed high expression of α(1,2)-linked fucosylated proteins compared to normal ST. The expression of α(1,2)-linked fucosylated monocyte chemoattractant protein 1 (MCP-1)/CCL2 was significantly elevated in RA SF compared with osteoarthritis SF. Depletion of α(1,2)-linked fucosylated proteins in RA SF induced less HMVEC migration and tube formation than occurred in sham-depleted RA SF. We found that blocking FUT1 expression in ECs resulted in decreased MCP-1/CCL2 and RANTES/CCL5 production. Finally, we showed that FUT1 regulates EC migration in response to vascular endothelial cell growth factor.**

Conclusion. **Our findings indicate that α(1,2)-linked fucosylation by FUT1 may be an important new target for angiogenic diseases such as RA.**

Posttranslational protein modification can lead to alteration of biologic properties of proteins (1,2). Glycosylation is one of these modifications, and many proteins are glycosylated in eukaryotes (3). For example, oligosaccharide antigens are used as tumor markers, and oligosaccharides in tumors modulate functions such as tumor cell adhesion and invasion (4). It has also been shown that the expression of sialyl-Lewis^x is elevated in gastric cancers, and several antibodies raised against sialyl-Lewis^x are used for the diagnosis of cancers (4). Fucosylation of glycoproteins involves the biologic functions of adhesion molecules and growth factor receptors (5). Fucosylated glycans are synthesized by 13 fucosyltransferases (FUTs). Terminal fucose can be linked to α(1,2)-, α(1,3)-, α(1,4)-, or α(1,6)-orientations by these FUTs. In addition, expression of FUTs has been reported in some cancers, such as prostate and pancreatic cancer (6,7).

FUT1 and FUT2 are α(1,2)-fucosyltransferases responsible for synthesis of the H blood group antigen (8,9). The expression of cancer-associated carbohydrate antigens is modified by abnormal control by glycosyltransferases. We have previously shown that the soluble form of E-selectin mediates angiogenesis via its endo-

Supported by the Office of Research and Development, Medical Research Service, Department of Veterans Affairs and by the Frederick G. L. Huetwell and William D. Robinson, MD, Professorship in Rheumatology at the University of Michigan (awarded to Dr. Koch).

[1]Takeo Isozaki, MD, PhD, Mohammad A. Amin, MD, Jeffrey H. Ruth, PhD, Phillip L. Campbell, BA, Pei-Suen Tsou, PhD, Christine M. Ha, BS, W. Alex Stinson, BS, Steven E. Domino, MD, PhD: University of Michigan, Ann Arbor; [2]Alisa E. Koch, MD: Department of Veterans Affairs Medical Center, Ann Arbor and University of Michigan, Ann Arbor.

Drs. Isozaki, Amin, and Ruth contributed equally to this work.

Dr. Domino has received a one-time licensing fee from Pfizer for fucosyltransferase-mutant mice.

Address correspondence to Alisa E. Koch, MD, 4002 Calgary Court, Ann Arbor, MI 48108. E-mail: aekoch@umich.edu.

Submitted for publication March 19, 2013; accepted in revised form March 25, 2014.

thelial ligand sialyl-Lewis^x (10), and that a related antigen, Lewis^y-6/H/5-2 (Le^y/H), which is synthesized by FUT1, and its glucose analog 2-fucosyllactose, mediate angiogenesis and inflammatory cell adhesion (11,12).

Progression of rheumatoid arthritis (RA) is characterized by the appearance of inflammatory cells in both the pannus and joint fluid and by eventual tissue destruction. The RA synovium contains elevated levels of proangiogenic cytokines and inflammatory cells, such as lymphocytes and monocytes (13,14). One of the most effective current therapies is designed to block tumor necrosis factor α (TNFα) (15). Some TNFα-blocking biologic agents are composed of IgG, and glycosylation in the Fc region plays an important role in the stability and effectiveness of such therapeutics (16).

Angiogenesis is critical in vasculoproliferative processes, including tumor growth, and inflammatory states such as psoriasis and RA (17). The process of angiogenesis contributes to RA progression and may be an appropriate therapeutic target (18). In this study, we demonstrate the expression of α(1,2)-linked fucosylated proteins in RA and their role in angiogenesis and cell recruitment. We also show that blocking FUT1 in endothelial cells (ECs) reduces production of proangiogenic chemokines and EC migration.

MATERIALS AND METHODS

Patients. RA and osteoarthritis (OA) synovial tissue (ST) samples were obtained from patients undergoing arthroplasty or synovectomy. Normal ST samples were obtained from a National Disease Research Interchange and Cooperative Human Tissue Network. RA and OA synovial fluid (SF) samples were obtained from the patients. Normal skin tissue samples were obtained from the University of Michigan Tissue Procurement Service. All specimens were collected following approval by the University of Michigan Institutional Review Board.

Generation of FUT1 gene–deficient mice. FUT1 gene–deficient mice have been generated previously (19–21). Mice were viable without gross defects, and were bred onto a C57BL/6 background (19–21). FUT1 gene–deficient mice were later obtained from the Consortium for Functional Glycomics. C57BL/6 wild-type mice were bred in-house or purchased from the National Cancer Institute. All animal experiments were approved by the University of Michigan Committee on Use and Care of Animals.

Cell culture. Human dermal microvascular endothelial cells (HMVECs) were purified from digested skin tissue specimens using mouse anti-human CD31 MicroBeads according to the recommendations of the manufacturer (Miltenyi Biotec). Cells were cultured in EC basal medium (Lonza) with all growth factors. In order to confirm EC purification, we examined EC markers on these cells using antibodies to von Willebrand factor (vWF) and CD31.

Isolation and confirmation of EC purity in mouse lung preparations. Mouse lung ECs were harvested from wild-type and FUT1 gene–deficient mouse lungs using rat anti-mouse CD146 MicroBeads according to the recommendations of the manufacturer (Miltenyi Biotec), and cultured in EC basal medium with all growth factors (Lonza) (22).

Flow cytometry. In order to confirm mouse lung EC purity, we performed flow cytometry using fluorescein isothiocyanate (FITC)–conjugated CD146 antibody (Miltenyi Biotec). Mouse lung ECs (3×10^6 cells/ml) were suspended in blocking buffer and incubated for 15 minutes at 4°C. The cells were incubated with rat FITC-conjugated IgG or FITC-conjugated CD146 for 30 minutes at 4°C. Flow cytometry was performed as previously described (23).

Cell treatment. HMVECs and mouse lung ECs were seeded in 6-well plates (BD Biosciences) at a density of 2×10^5 cells per well. Cells were then maintained in EC basal medium with 5% fetal bovine serum (FBS). After overnight serum starvation, cells were treated with TNFα (25 ng/ml; R&D Systems) for various time periods or interleukin-1β (IL-1β) (25 ng/ml; R&D Systems) as previously described (24,25). Cell-conditioned medium was collected and used in assays.

Immunofluorescence staining. Immunofluorescence staining was performed as previously described (26). To determine if α(1,2)-linked fucosylated proteins were expressed on RA, OA, and normal ST ECs, rabbit anti-human vWF (Dako) and goat anti–*Ulex europaeus* agglutinin type I (anti–UEA-I; Vector) were used. RA, OA, and normal ST slides were fixed with cold acetone for 20 minutes. Then slides were blocked with 20% FBS and 5% donkey serum for 1 hour at 37°C, and incubated with UEA-I (2 μg/ml; Vector) for 1 hour at 37°C. UEA-I binds specifically to α(1,2)-fucose, the terminal sugar of blood group antigens H and Lewis^y. Goat anti–UEA-I and rabbit anti-human vWF were used as primary antibodies. Fluorescence-conjugated donkey anti-goat (for UEA-I) and anti-rabbit (for vWF) secondary antibodies were purchased from Life Technologies. DAPI was used for nuclear staining. Images were obtained at 200× magnification. Anti-vWF–positive vessels were shown by fluorescent green staining, and fucosylation was shown by fluorescent red staining. Yellow vessels were a result of the merger of the green and red fields. We determined the percentage of α(1,2)-fucosylated vessels in RA, OA, and normal ST by counting the total number of yellow vessels, and divided this value by the total number of vessels (green) in each tissue section. Each section was evaluated by an observer who was blinded with regard to the experimental conditions.

Depletion of rheumatoid factor (RF) from SF. To avoid any possible confounding effects of RF on assays, RF was immunodepleted from SF samples using anti-IgM antibodies coupled to agarose beads (Sigma-Aldrich) as previously described (23). Removal of RF was determined by randomly choosing 6 RA SF samples and measuring RF levels before and after immunodepletion using an RF enzyme-linked immunosorbent assay (ELISA) kit (Alpha Diagnostic). Before immunodepletion, RF levels were measured and ranged from 21 IU/ml to 132 IU/ml. After immunodepletion, all samples had RF levels $<$10 IU/ml (data not shown).

Immunoprecipitation and lectin blotting. RF-depleted RA SF and OA SF samples were incubated with mouse anti-human monocyte chemoattractant protein 1 (MCP-1)/

CCL2 antibody (R&D Systems) for 2 hours. The antibody–protein complexes were incubated with protein A–agarose beads (Millipore) overnight at 4°C. The next day, antibody–protein–agarose bead complexes were washed 5 times with Tris buffered saline (TBS; 50 m*M* Tris Cl [pH 7.6] and 150 m*M* NaCl), and resuspended in Laemmli sample buffer.

For lectin blotting, samples were loaded onto two 10% polyacrylamide gels under reducing conditions. One gel was stained with Coomassie brilliant blue R250 (Bio-Rad). The other gel was electrotransferred onto a PVDF membrane. After transfer, the membrane was washed with TBS containing 0.05% Tween 20 (TBST), blocked with 2% bovine serum albumin in TBST overnight at 4°C, and incubated with 5 μg/ml of biotinylated UEA-I (Vector) for 1 hour at room temperature. After washing with TBST, the blot was incubated with streptavidin–horseradish peroxidase (HRP) diluted 1:50,000 (BD Biosciences) for 1 hour at room temperature. Finally, the blot was washed with TBST and the color was developed using a BCIP/NBT Liquid Substrate System (Sigma-Aldrich). As a loading control, the blots were stripped and probed with an anti–MCP-1/CCL2 antibody (R&D Systems). Densitometric analysis of the bands was performed using Un-Scan-It software, version 5.1 (Silk Scientific).

Neutralization of α(1,2)-linked fucosylated proteins in RA SF. To determine the role of α(1,2)-linked fucosylated proteins in RA SF, RA SF samples were depleted using UEA-I–conjugated agarose beads (Vector). RA SF samples (1:50 diluted with phosphate buffered saline [PBS]) were mixed overnight with UEA-I–conjugated or nonspecific agarose beads (Sigma-Aldrich). The following day, SF samples were centrifuged to pellet the lectin glycoprotein complex, and depleted SF supernatants were collected. Depletion of α(1,2)-linked fucosylated proteins was confirmed by lectin blotting.

ELISAs for MCP-1/CCL2 and RANTES/CCL5. ELISAs were performed as previously described (23). To determine α(1,2)-linked fucosylated MCP-1/CCL2 and total MCP-1/CCL2 in RA SF samples, we measured MCP-1/CCL2 from sham-depleted and α(1,2)-linked fucosylated protein–depleted SF samples by using UEA-I–conjugated agarose beads. We quantitated α(1,2)-linked fucosylated MCP-1/CCL2 in SF samples by measuring total MCP-1/CCL2 in SF samples that were either sham depleted or depleted of α(1,2)-linked fucosylated proteins with UEA-I–conjugated agarose beads, as described above. Differences in the values of the sham-depleted and α(1,2)-linked fucosylated protein–depleted SF samples gave the value of α(1,2)-linked fucosylated MCP-1/CCL2 in SF samples. Levels of MCP-1/CCL2 and RANTES/CCL5 in TNFα-stimulated or IL-1β–stimulated HMVEC-conditioned medium were measured according to the recommendations of the manufacturer (R&D Systems). Levels of MCP-1/CCL2 and RANTES/CCL5 in TNFα-stimulated or IL-1β–stimulated mouse lung EC–conditioned medium were measured by personnel at the University of Michigan Cancer Center Immunology Core or using ELISA kits from commercial sources (R&D Systems).

In vitro HMVEC chemotaxis assay. Chemotaxis assays were performed using a 48-well modified Boyden chamber system as previously described (23,27). To examine the bioactivity of α(1,2)-linked fucosylated proteins in RA SF samples, we performed HMVEC chemotaxis assays using α(1,2)-linked fucosylated protein–depleted or sham-depleted RA SF samples. Each test group was assayed in quadruplicate. Three high-power (400×) fields were counted in each replicate well, and results were expressed as cells per high-power field (hpf).

In vitro Matrigel tube formation assay. Matrigel tube formation assays using growth factor–reduced Matrigel (BD Biosciences) were performed (28,29). To examine the bioactivity of α(1,2)-linked fucosylated proteins in RA SF samples, we performed HMVEC tube formation assays using α(1,2)-linked fucosylated protein–depleted or sham-depleted RA SF samples. The controls used were vascular endothelial cell growth factor (VEGF) (10 n*M*; R&D Systems) as a positive control and PBS as a negative control. HMVECs (1.8×10^4 cells/400 μl) were plated on Matrigel in the presence of 150 μg/ml sham-depleted or α(1,2)-linked fucosylated protein–depleted RA SF for 6 hours at 37°C. Photographs (100×) were obtained, and tubes were counted in a blinded manner. Tubes were defined as elongated connecting branches between two identifiable HMVECs.

After finding that FUT1 plays an important role in TNFα-induced MCP-1/CCL2 and RANTES/CCL5 secretion, we examined whether MCP-1/CCL2 and RANTES/CCL5 were involved in TNFα-mediated tube formation. We performed HMVEC tube formation assays using TNFα as a stimulus in the presence or absence of neutralizing antibodies against MCP-1/CCL2 and RANTES/CCL5 (R&D Systems).

Oligonucleotide (ODN) transfection. HMVECs were seeded in 6-well plates at 1×10^5 cells per well. ECs were maintained in EC basal medium with 5% FBS. Upon 70% confluency, 2 μg/ml FUT1 sense or antisense ODNs and TransIT-Oligo transfection reagent (Mirus) was mixed according to the manufacturer's instructions and overlaid on the cells. Cells were incubated with the ODNs/TransIT-Oligo transfection reagent for 24 hours at 37°C. FUT1 sense and antisense ODNs were purchased from Integrated DNA Technologies. The following FUT1 sequences were used: for FUT1 sense ODN, TTTCTTCCACCATCTCCGGGAA and for FUT1 antisense ODN, CCTTCTCTCCAACTCTCCCA. The percent knockdown of FUT1 expression was determined by quantitative polymerase chain reaction (qPCR).

RNA extraction and qPCR. RNA extraction and qPCR were performed as previously described (30). Total RNA was isolated from HMVECs transfected with sense or antisense ODNs directed against FUT1, using RNeasy Mini RNA isolation kits in conjunction with QIAshredder, following the recommendations of the manufacturer (Qiagen). Using this technique, we routinely yield ~40 ng/μl of RNA from 1×10^5 cells. Following isolation, RNA (2 μl) was quantified and checked for purity using a spectrophotometer (NanoDrop Technologies). FUT1 and β-actin primer pairs were purchased from Integrated DNA Technologies. The following primers were used: for FUT1, forward 5′-GTGCCCGTATCCAGAGTGAT-3′ and reverse 5′-AGGACCCAGGGGAGAGTAAA-3′; for β-actin, forward 5′-GCTAGGCAGCTCGTAGCTCT-3′ and reverse 5′-GCCATGTACGTTGCTATCCA-3′. All samples were run in duplicate and analyzed using Applied Biosystems software (Life Technologies).

EC chemotaxis with FUT1 gene–deficient and wild-type mouse lung ECs. Mouse lung ECs (from passages 2–4) were maintained in EC basal medium (Lonza) and 5% FBS. For the assay, the cells were fed one night before with EC basal medium with 5% FBS, harvested, and resuspended at 5×10^5

cells/ml in EC basal medium with 0.1% FBS. EC chemotaxis assays were performed using gelatin-coated polycarbonate membranes (8 μm pore size) (28,29). The chambers were inverted and incubated for 2 hours to allow mouse EC attachment. The chambers were reinverted, test substances were added, and incubation was continued for 1 additional hour. VEGF (Life Technologies) was used as a stimulus, and PBS was used as a negative control.

HMVEC chemotaxis assay with FUT1 sense or antisense ODN–transfected EC–conditioned medium. To further examine the role of FUT1 in ECs, we performed HMVEC chemotaxis assays using FUT1 sense or antisense ODN-transfected HMVEC-conditioned medium to determine whether HMVEC FUT1 inhibition alters the secretion of chemotactic substances by cultured ECs. We used PBS as a negative control and VEGF (10 n*M*; R&D Systems) as a positive control for these studies.

Cell lysis and immunoblotting with mouse lung ECs. Cell lysis and immunoblotting were performed as previously described (29). Wild-type and FUT1 gene–deficient mouse lung ECs were stimulated with TNFα (25 ng/ml) for various time periods. At the end of each time period, cell lysates were prepared. The protein concentration in all of the samples was measured with a bicinchoninic acid protein assay kit (Pierce). Protein lysates (10 μg) were run on 10% sodium dodecyl sulfate–polyacrylamide gels and transblotted onto nitrocellulose membranes (Bio-Rad). Blots were probed for rabbit anti-mouse antibodies for various VEGF receptors (VEGFRs). Blots were stripped and reprobed with β-actin to verify equal loading of proteins.

Statistical analysis. Data were analyzed using Student's *t*-test, assuming equal variances. Data are reported as the mean ± SEM. *P* values less than 0.05 were considered significant.

RESULTS

Expression of α(1,2)-linked fucosylated proteins on RA ST endothelial cells. We examined the expression of α(1,2)-linked fucosylated proteins in RA, OA, and normal ST samples. We used UEA-I and antibody to UEA-I for immunohistology, because UEA-I binds specifically to α(1,2)-fucose (31). We found that α(1,2)-linked fucosylated proteins were expressed on ST ECs (Figure 1A). In addition, α(1,2)-linked fucosylated proteins were highly expressed in RA ST compared to normal ST (mean ± SEM percent α(1,2)-linked fucosylated protein–positive tubes of total tubes 60 ± 6% versus 32 ± 9%; $P < 0.05$) (Figure 1B). These results suggest that α(1,2)-linked fucosylation may be important for EC angiogenic activity in RA ST.

Expression of α(1,2)-linked fucosylated chemokines in RA SF. We and others have shown chemokines to be important in RA (32–34). To determine if α(1,2)-linked fucosylated chemokines were present in RA, we performed α(1,2)-linked fucosylated MCP-1/CCL2 immunoprecipitation studies. Figure 2A shows α(1,2)-linked fucosylated MCP-1/CCL2 in RA and OA SF. We found that the expression of α(1,2)-linked fucosylated MCP-1/CCL2 was significantly elevated in RA SF compared to OA SF (Figure 2B). In order to measure

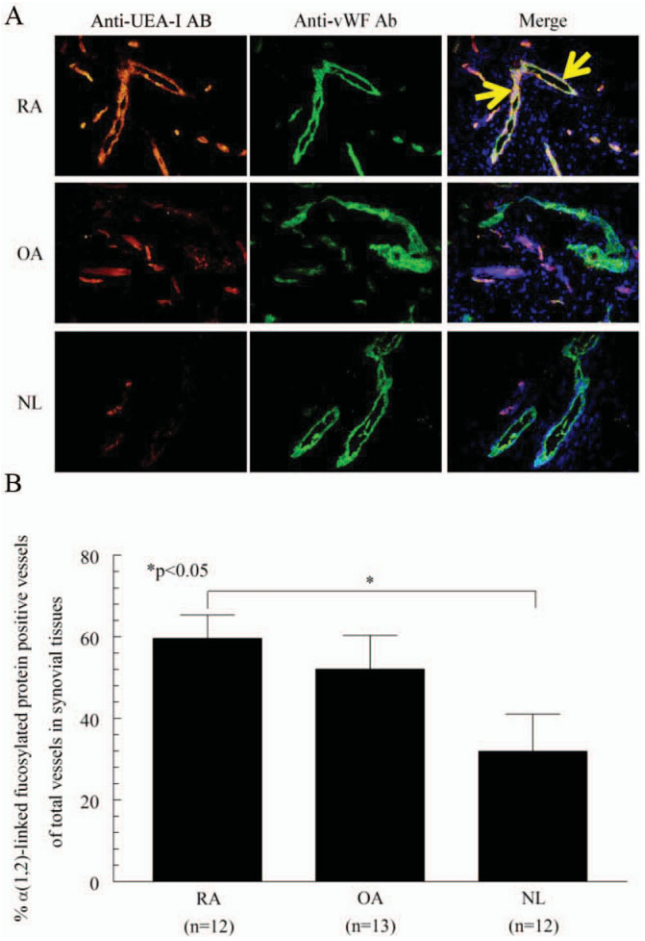

Figure 1. Expression of α(1,2)-linked fucosylated proteins in rheumatoid arthritis (RA), osteoarthritis (OA), and normal (NL) synovial tissue (ST) endothelial cells (ECs). **A**, ST staining with *Ulex europaeus* agglutinin type I (UEA-I) and goat anti–UEA-I antibody (Ab) (left), staining with rabbit anti–von Willebrand factor (anti-vWF) antibody (middle), and merge of the anti–UEA-I and anti-vWF stainings (right). Yellow indicates α(1,2)-linked fucosylated proteins associated with ST ECs. **Arrows** indicate α(1,2)-linked fucosylated protein–positive ECs. Original magnification × 200. **B**, Percentages of α(1,2)-linked fucosylated protein–positive vessels in RA, OA, and normal ST, determined by counting the total number of yellow vessels and dividing that value by the total number of vWF-positive vessels (green) in each tissue section. RA ST had significantly higher percentages of α(1,2)-linked fucosylated protein–containing vessels compared to normal ST. IgG control staining for all 3 groups did not show staining (results not shown). Bars show the mean ± SEM. The n values are the number of patients.

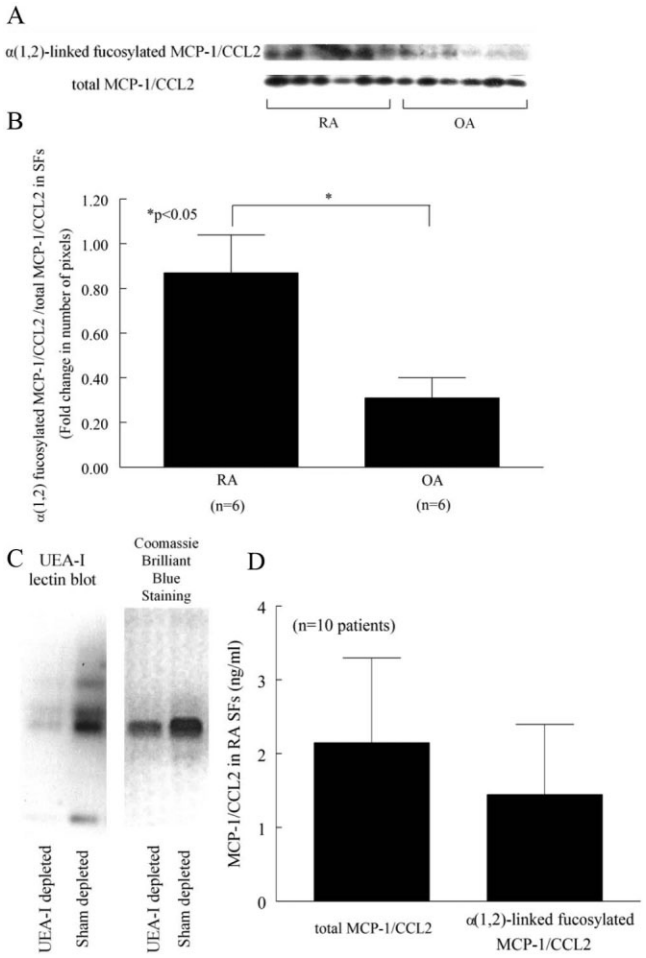

Figure 2. Expression of α(1,2)-linked fucosylated monocyte chemoattractant protein 1 (MCP-1)/CCL2 in synovial fluid (SF). **A**, Detection of α(1,2)-linked fucosylated MCP-1/CCL2 in SF samples from 6 RA patients and 6 OA patients, by immunoprecipitation and lectin blotting. **B**, Levels of α(1,2)-linked fucosylated MCP-1/CCL2 in RA SF and OA SF. There was a significant elevation of α(1,2)-linked fucosylated MCP-1/CCL2 in RA SF. Data were normalized to total MCP-1/CCL2 and are the ratio of the densitometry of α(1,2)-linked fucosylated MCP-1/CCL2 to total MCP-1/CCL2 shown in **A**. The n values are the number of patients. **C**, Left, Depletion of α(1,2)-linked fucosylated proteins in RA SF using UEA-I–conjugated agarose beads, as shown by lectin blotting. Right, Coomassie brilliant blue staining. The α(1,2)-linked fucosylated proteins are decreased after depletion. **D**, Levels of MCP-1/CCL2 in sham-depleted and α(1,2)-linked fucosylated protein–depleted RA SF, as measured using an MCP-1/CCL2 enzyme-linked immunosorbent assay. The mean ± SEM percent α(1,2)-linked fucosylated MCP-1/CCL2 of total MCP-1/CCL2 was 76 ± 9%. Bars in **B** and **D** show the mean ± SEM. See Figure 1 for other definitions.

α(1,2)-linked fucosylated MCP-1/CCL2 in RA SF, SF samples were depleted of α(1,2)-linked fucosylated proteins using UEA-I–conjugated agarose beads. We then determined whether α(1,2)-linked fucosylated proteins were depleted in SF by lectin blotting. We confirmed that the expression of α(1,2)-linked fucosylated proteins was decreased after depletion (Figure 2C). We then measured MCP-1/CCL2 by ELISA. The mean ± SEM values for α(1,2)-linked fucosylated MCP-1/CCL2 and total MCP-1/CCL2 in RA SF were 1.4 ± 1.0 ng/ml and 2.1 ± 1.2 ng/ml, respectively (n = 10 patients) (Figure 2D). The percent of α(1,2)-linked fucosylated MCP-1/CCL2 of total MCP-1/CCL2 was 76 ± 9% (n = 10 patients). These results indicate that α(1,2)-linked fucosylated MCP-1/CCL2 is found in SF and is up-regulated in RA SF compared to OA SF.

Function of α(1,2)-linked fucosylated proteins in RA SF. In order to demonstrate the function of α(1,2)-linked fucosylated proteins in RA SF, SF samples neutralized of α(1,2)-linked fucosylated proteins were assayed for the ability to induce HMVEC chemotaxis and tube formation. Because EC chemotaxis is an initial step in the angiogenic process, we performed in vitro HMVEC chemotaxis assays using sham-depleted or α(1,2)-linked fucosylated protein–depleted RA SF. We found that α(1,2)-linked fucosylated protein–depleted RA SF samples (n = 4 patients) showed a 54 ± 2% decrease in EC migratory activity compared to sham-depleted controls (mean ± SEM number of HMVECs migrated 8 ± 1 versus 17 ± 2; $P < 0.05$) (Figure 3A). In addition, α(1,2)-linked fucosylated protein–depleted RA SF samples (n = 4 patients) showed a 50 ± 21% decrease in EC tube-forming activity compared to sham-depleted controls (mean ± SEM number of HMVEC tubes formed 6 ± 2 versus 12 ± 1; $P < 0.05$) (Figure 3B).

Figure 3C shows a representative image of Matrigel in vitro. The total length of the tubes formed and the number of nodes formed showed a similar trend. There was a 72 ± 7% decrease in total length of the tubes formed in α(1,2)-linked fucosylated protein–depleted RA SF samples compared to sham-depleted controls (mean ± SEM length 21 ± 6 mm versus 71 ± 4 mm; $P < 0.05$) (results not shown). There was a 75 ± 13% decrease in the number of nodes in α(1,2)-linked fucosylated protein–depleted RA SF samples compared to sham-depleted controls (mean ± SEM 2 ± 1 versus 6 ± 0; $P < 0.05$) (Figure 3C). These findings suggest that α(1,2)-linked fucosylated proteins in RA SF have more potent EC angiogenic activity compared to non–α(1,2)-linked fucosylated proteins. After finding that the production of MCP-1/CCL2 was decreased in FUT1 gene–deficient mouse lung ECs compared to wild-type mouse lung ECs, we examined if MCP-1/CCL2 was involved in TNFα-mediated tube formation in HMVECs. We found

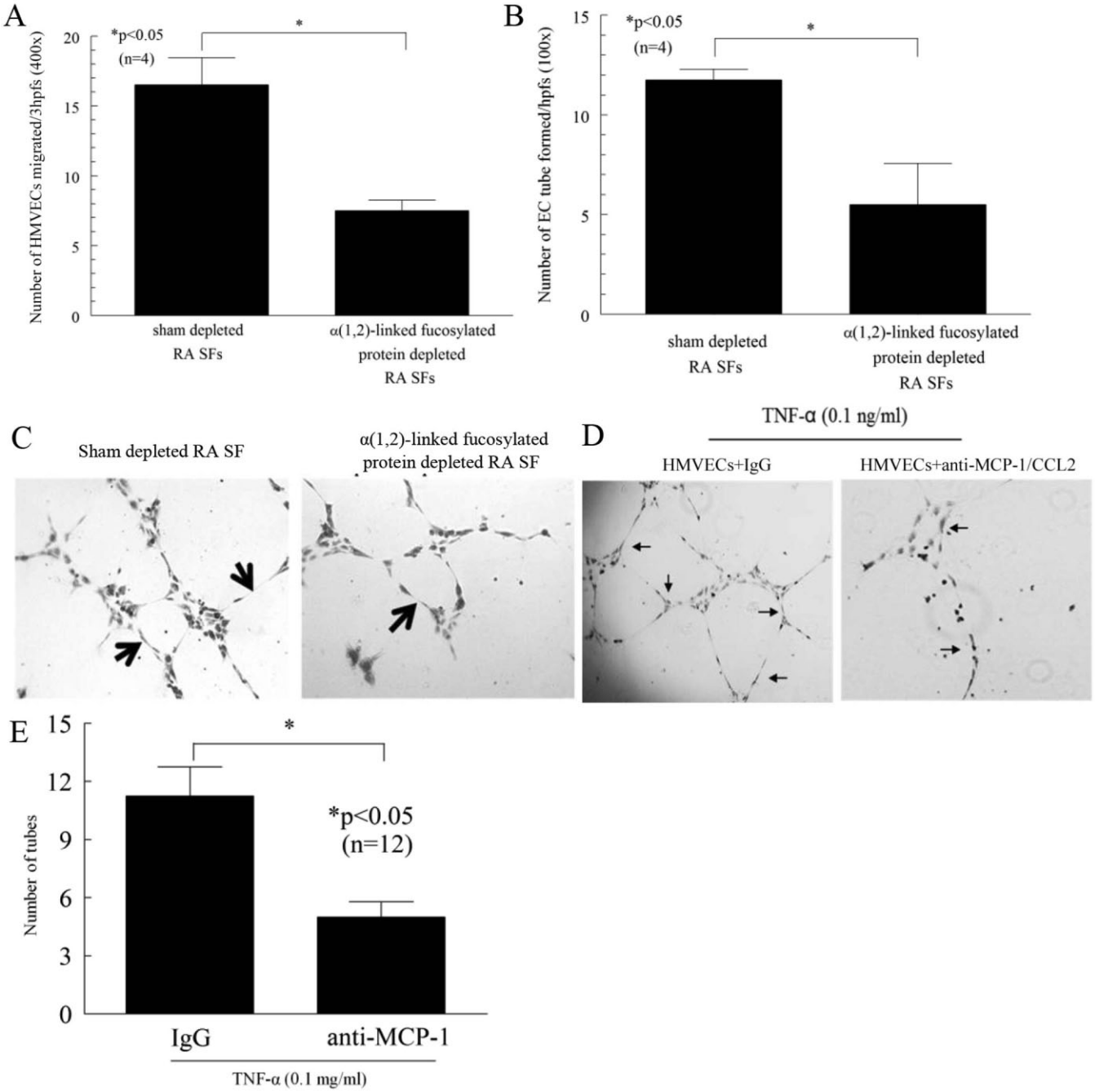

Figure 3. Chemotactic and tube formation activity of α(1,2)-linked fucosylated proteins in rheumatoid arthritis (RA) synovial fluid (SF). **A**, Number of migrated human dermal microvascular endothelial cells (HMVECs) in sham-depleted and α(1,2)-linked fucosylated protein–depleted RA SF. HMVEC migration was measured using a chemotaxis assay. Depletion of α(1,2)-linked fucosylated protein resulted in a mean ± SEM 54 ± 2% reduction in RA SF–induced HMVEC migration. **B**, Number of tubes formed in sham-depleted and α(1,2)-linked fucosylated protein–depleted RA SF. There was less HMVEC tube-forming activity in α(1,2)-linked fucosylated protein–depleted RA SF. **C**, HMVEC tubes formed by sham-depleted and α(1,2)-linked fucosylated protein–depleted RA SF. **Arrows** indicate tubes. Original magnification × 100. **D** and **E**, Inhibition of tumor necrosis factor α (TNFα)–mediated HMVEC tube formation on Matrigel by blocking antibody against monocyte chemoattractant protein 1 (MCP-1)/CCL2. **Arrows** indicate the number of tubes formed. Original magnification × 40 in **D**. Bars in **A**, **B**, and **E** show the mean ± SEM. The n values in **A** and **B** are the number of patients; the n values in **E** are the number of replicates.

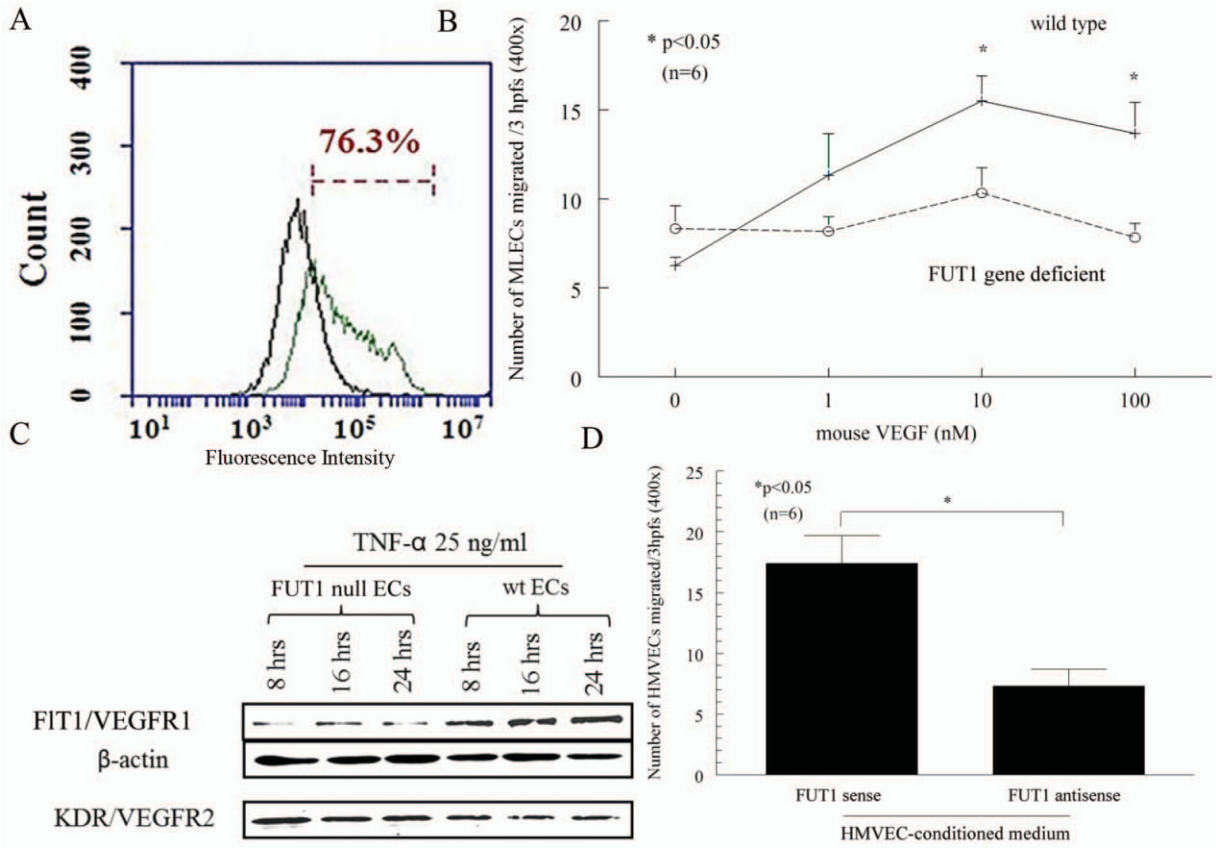

Figure 4. **A**, Purity of wild-type mouse lung endothelial cells (MLECs), as determined by flow cytometry. The purity of C57BL/6 wild-type (WT) mouse lung ECs was 76.3%, as determined by CD146 staining via flow cytometric analysis. Blocking fucosyltransferase 1 (FUT1) in ECs reduced EC chemotaxis. Green represents CD146-positive cells; black represents control IgG. Results are representative of 2 independent assays. **B**, Reduction in cell migration in ECs completely lacking FUT1 expression. FUT1 gene–deficient mouse lung ECs had significantly less migration compared to wild-type mouse lung ECs in response to mouse vascular endothelial cell growth factor (VEGF; 10 n*M* and 100 n*M*). hpfs = high-power fields. The n value is the number of experiments. **C**, Marked increase in Flt1/VEGF receptor 1 (VEGFR1) induced by tumor necrosis factor α (TNFα; 25 ng/ml) in wild-type mouse lung ECs compared to FUT1 gene–deficient mouse lung ECs at 8, 16, and 24 hours. Results are representative of 2 independent assays. KDR = kinase insert domain receptor. **D**, FUT1 antisense oligonucleotide (ODN)–transfected HMVEC–conditioned medium reduces HMVEC migration compared to FUT1 sense ODN–transfected HMVEC–conditioned medium. Phosphate buffered saline (PBS) and VEGF were used as negative and positive controls, respectively. The mean ± SEM number of HMVECs migrating toward PBS was 5 ± 1 and the number migrating toward VEGF was 40 ± 6. Bars show the mean ± SEM. The n value is the number of experiments. Color figure can be viewed in the online issue which is available at http://onlinelibrary.wiley.com/doi/10.1002/art.38648/abstract.

that TNFα-induced HMVEC tube formation was significantly decreased in the presence of neutralizing antibody to MCP-1/CCL2, suggesting that MCP-1/CCL2 is involved, in part, in TNFα-stimulated angiogenesis (Figures 3D and E). We did not see a similar effect with RANTES, suggesting that this chemokine is regulated differently than MCP-1/CCL2 in this system (data not shown).

Validation of the purity of the mouse lung ECs by flow cytometry. To validate the purity of the EC population, flow cytometry was performed using FITC-conjugated CD146, a mouse EC marker. ECs were 76% CD146 positive (Figure 4A).

Decreased EC chemotaxis in FUT1 gene–deficient mouse lung ECs versus wild-type ECs. To determine the role of FUT1 in angiogenesis, we performed in vitro chemotaxis assays. FUT1 gene–deficient and wild-type mouse lung ECs were assayed for their chemotactic response to VEGF, in a modified Boyden chamber. We found that FUT1 gene–deficient mouse lung ECs showed decreased migration toward VEGF compared to wild-type mouse lung ECs (mean ± SEM

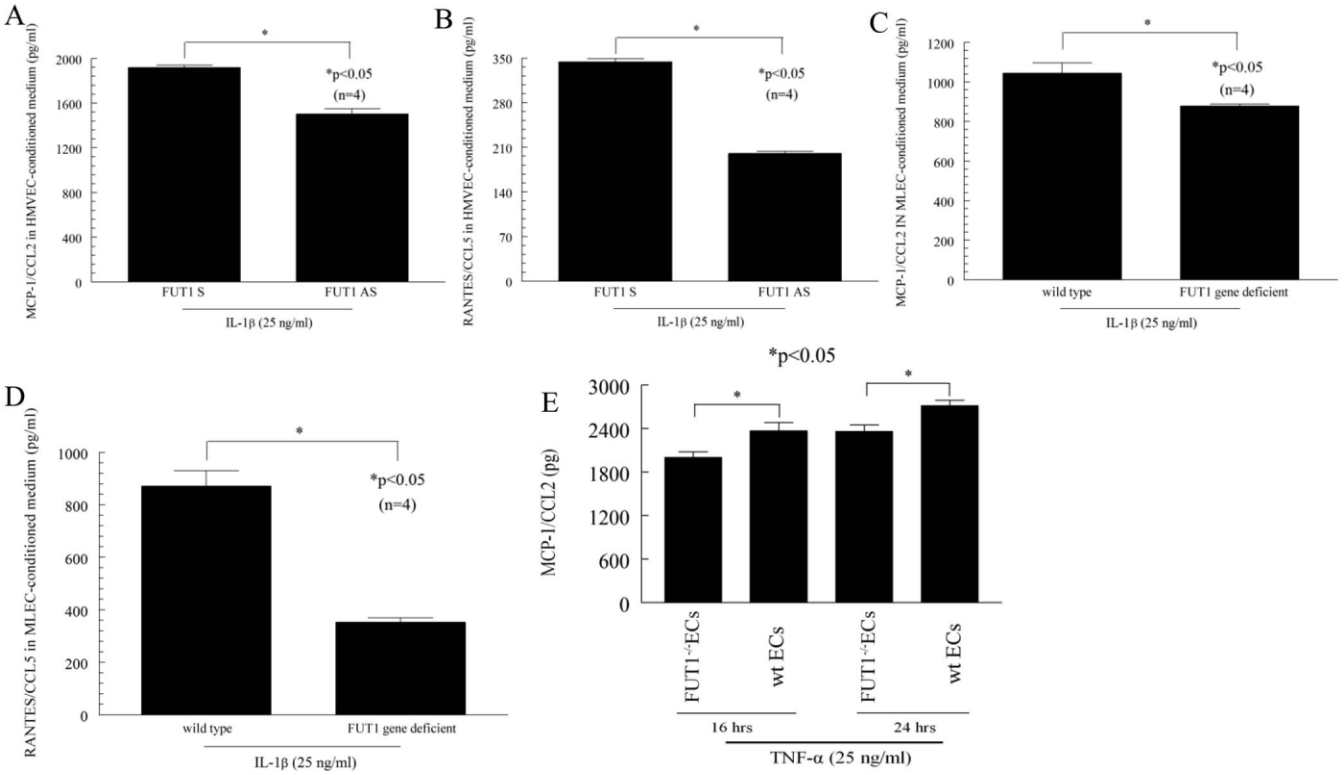

Figure 5. Reduction in expression of proangiogenic chemokines by blocking FUT1 expression in ECs. Cells were treated with interleukin-1β (IL-1β) for 72 hours, and conditioned medium was assayed. **A**, Levels of monocyte chemoattractant protein 1 (MCP-1)/CCL2 in human dermal microvascular endothelial cell (HMVEC)–conditioned medium transfected with FUT1 sense (S) ODN or FUT1 antisense (AS) ODN and stimulated with IL-1β. There was a mean ± SEM 21 ± 3% decrease in MCP-1/CCL levels in HMVEC-conditioned medium transfected with FUT1 antisense ODN. **B**, Levels of RANTES/CCL5 in HMVEC-conditioned medium transfected with FUT1 sense ODN or FUT1 antisense ODN and stimulated with IL-1β. There was a mean ± SEM 41 ± 0% decrease in RANTES/CCL5 levels in HMVEC-conditioned medium transfected with FUT1 antisense ODN. **C**, Levels of MCP-1/CCL2 in wild-type and FUT1 gene–deficient mouse lung EC–conditioned medium stimulated with IL-1β. There was a mean ± SEM 15 ± 5% decrease in MCP-1/CCL2 levels in FUT1 gene–deficient mouse lung EC–conditioned medium. **D**, Levels of RANTES/CCL5 in wild-type and FUT1 gene–deficient mouse lung EC–conditioned medium stimulated with IL-1β. There was a mean ± SEM 59 ± 1% decrease in RANTES/CCL5 levels in FUT1 gene–deficient mouse lung EC–conditioned medium. **E**, MCP-1/CCL2 expression induced by tumor necrosis factor α (TNFα) in FUT1 gene–deficient and wild-type mouse lung ECs after 16 and 24 hours. TNFα expression was significantly lower in FUT1 gene–deficient mice at both time points. Bars show the mean ± SEM. The n values are the number of replicates. See Figure 4 for other definitions.

number of mouse lung ECs migrated 10 ± 1 versus 16 ± 1 at 10 n*M* [n = 6] and 8 ± 1 versus 14 ± 2 at 100 n*M* [n = 6]; $P < 0.05$) (Figure 4B). After finding that VEGF induces migration of mouse lung ECs, we examined the expression of angiogenic VEGFRs in FUT1 gene–deficient and wild-type mouse lung ECs. We found that Flt1/VEGFR-1 levels were markedly increased in a time-dependent manner in wild-type mouse lung ECs stimulated with TNFα compared to FUT1 gene–deficient mouse lung ECs stimulated with TNFα. This suggests a mechanism by which FUT1 gene–deficient mouse lung ECs migrate less in response to VEGF (Figure 4C). However, we did not find a decrease in levels of kinase insert domain receptor/VEGFR-2, another receptor for VEGF, in response to TNFα in FUT1 gene–deficient mouse lung ECs compared to wild-type mouse lung ECs (Figure 4C).

Reduction in EC migration to conditioned medium upon blocking of FUT1 expression in ECs. To further examine the function of FUT1 in ECs, we used HMVECs transfected with sense or antisense ODNs directed against FUT1. The mean ± SEM percent knockdown of FUT1 in antisense ODN–transfected HMVECs was 41 ± 7% (n = 3). We performed HMVEC chemotaxis toward FUT1 sense ODN– or antisense ODN–transfected HMVEC–conditioned me-

dium and found that FUT1 antisense ODN–transfected HMVEC–conditioned medium showed a significant decrease in the chemotactic activity of HMVECs compared to FUT1 sense ODN–transfected HMVEC–conditioned medium (mean ± SEM number of HMVECs migrated 7 ± 1 versus 17 ± 2; $P < 0.05$) (Figure 4D).

Reduction in expression of proangiogenic chemokines upon blocking of FUT1 expression in ECs. To determine whether angiogenic chemokines were present in EC-conditioned medium and whether their expression was regulated by proinflammatory cytokines, ELISAs were performed on conditioned medium. HMVECs were transfected with FUT1 antisense ODNs and then stimulated with IL-1β to induce chemokine production. This conditioned medium contained much lower levels of MCP-1/CCL2 than medium from sense-transfected HMVECs when stimulated with IL-1β (Figure 5A). (The mean ± SEM level of MCP-1/CCL2 was 1,578 ± 35 pg/ml for unstimulated medium transfected with FUT1 sense ODN versus 343 ± 30 pg/ml for unstimulated medium transfected with FUT1 antisense ODN; n = 4 replicates.) RANTES/CCL5 levels were also decreased in response to IL-1β in FUT1 antisense ODN–transfected HMVEC–conditioned medium compared to FUT1 sense ODN–transfected HMVEC–conditioned medium (Figure 5B). (The mean ± SEM level of RANTES/CCL5 was 51 ± 2 pg/ml for unstimulated medium transfected with FUT1 sense ODN versus 44 ± 4 pg/ml for unstimulated medium transfected with FUT1 antisense ODN; n = 4 replicates.) (Figure 5B).

We also found that MCP-1/CCL2 levels were significantly decreased in IL-1β–stimulated FUT1 gene–deficient mouse lung EC conditioned medium compared to wild-type mouse lung EC conditioned medium (Figure 5C). (The mean ± SEM level of MCP-1/CCL2 was 316 ± 28 pg/ml for unstimulated wild-type mouse lung EC conditioned medium versus 302 ± 79 pg/ml for unstimulated FUT1 gene–deficient mouse lung EC conditioned medium; n = 4 replicates.) RANTES/CCL5 levels were also significantly decreased in FUT1 gene–deficient mouse lung EC conditioned medium compared to wild-type mouse lung EC–conditioned medium in response to IL-1β (Figure 5D). (The mean ± SEM level of RANTES/CCL5 was 85 ± 22 pg/ml for unstimulated wild-type mouse lung EC–conditioned medium versus 9 ± 5 pg/ml for unstimulated FUT1 gene–deficient mouse lung EC–conditioned medium; n = 4 replicates.) However, expression of MCP-1/CCL2 and RANTES/CCL5 was not significantly decreased in conditioned medium when TNFα was used as a stimulus with similar culture conditions (data not shown). We also measured VEGF in FUT1 gene–deficient and wild-type mouse lung EC–conditioned medium, and did not find significant differences between FUT1 gene–deficient and wild-type mouse lung EC–conditioned medium (data not shown). These findings indicate that FUT1 inhibition can regulate CC chemokine production in ECs.

To examine the possibility that peak chemokine induction stimulated with TNFα may occur at a time point earlier than 24 hours, we measured the expression of MCP-1/CCL2 in conditioned media collected from FUT1 gene–deficient mouse lung ECs and wild-type mouse lung ECs stimulated with TNFα at 16 and 24 hours. TNFα induced significantly higher MCP-1/CCL2 secretion in wild-type mouse lung ECs compared to FUT1 gene–deficient mouse lung ECs at both 16 and 24 hours (Figure 5E). However, we did not see this difference at 8 hours (data not shown).

DISCUSSION

Glycosylation is involved in various events such as cell growth, cell migration, and tumor invasion. Approximately 50% of all proteins are glycosylated (35), suggesting that glycosylation is critical for proper protein function. Interestingly, it has also been shown that dysregulated protein glycosylation can lead to enhanced pathologic responses. For example, oligosaccharides on glycoproteins are altered during tumorigenesis, and play a role in regulating the metastatic potential of tumor cells (36).

Alpha-fetoprotein and prostate-specific antigen are commonly used tumor markers. However, elevated levels of these markers occur not only in cancer but also in benign diseases, whereas some groups reported that fucosylated tumor markers were more specific markers for active disease (6,37). The present study demonstrates that α(1,2)-linked fucosylated proteins are expressed in RA, and that the levels are highly elevated compared to levels in normal ST. We also show that α(1,2)-linked fucosylated MCP-1/CCL2 is present in RA SF, and that the levels are significantly elevated compared to levels in OA SF. Przybysz et al reported that the fucosylation of fibronectin in SF and blood plasma were related to RA progression (38). Ferens-Sieczkowska et al noted that fucosylation of synovial glycoconjugates could be a reliable clinical marker for RA and juvenile idiopathic arthritis (JIA) (39). All fucosylated proteins in RA, JIA, and traumatized knee SF samples were detected with *Aleuria aurantia*, one of the fucose-specific lectins. Fucosylated protein levels in RA and JIA were also ele-

vated compared to those in traumatized knee SF. However, no one has shown the role of fucosylation in RA. Our findings support the notion that α(1,2)-linked fucosylation is important in RA pathogenesis.

We examined the α(1,2)-linked fucosylation of MCP-1/CCL2 because this chemokine is an important monocyte chemotactic factor in RA and an angiogenic factor (32,33,40). We measured α(1,2)-linked fucosylated MCP-1/CCL2 using UEA-I–conjugated agarose beads, and found that the percent of α(1,2)-linked fucosylated MCP-1/CCL2 of total MCP-1/CCL2 in RA SF was 76 ± 9%. Our finding of elevated levels of α(1,2)-linked fucosylated MCP-1/CCL2 in RA SF suggests that posttranslational modification of this chemokine is increased in inflammatory environments such as the RA joint.

We previously found that FUT1 is expressed in the synovial lining of RA ST (41), and that α(1,2)-linked fucosylated proteins were overexpressed in RA. Because of this, we sought to determine whether these proteins in RA SF had chemotactic and angiogenic activity. We found that RA SF depleted of α(1,2)-linked fucosylated proteins induced less HMVEC migration compared to sham-depleted RA SF, suggesting that α(1,2)-linked fucosylation may have an important function in RA angiogenesis. Interestingly, Proost et al reported that glycosylated MCP-1/CCL2 was 2–3-fold less chemotactic for monocytes and THP-1 cells than nonglycosylated MCP-1/CCL2 (42). This discrepancy might be explained by the fact that they examined different cells and studied total glycosylation of MCP-1/CCL2, whereas we examined only α(1,2)-linked fucosylation. Carlyon et al reported that FUT4 gene– and FUT7 gene–deficient mouse neutrophils exhibited decreased secretion of the chemokines macrophage inflammatory protein 2/CXCL2 and keratinocyte-derived chemokine compared to wild-type mouse neutrophils (43). However, production of angiogenic chemokines in FUT1 gene–deficient ECs has not been demonstrated.

Mathieu et al reported that tumor vascularization was decreased after FUT1 inhibition (44), and supported the findings of Palumberi et al, who showed that adhesion of human epidermoid carcinoma cells to FUT1 and FUT2 small interfering RNA (siRNA)–transfected ECs was decreased compared to control siRNA–transfected ECs. These investigators also reported that FUT1 and FUT2 siRNA–treated human epidermoid carcinoma cells have reduced cell proliferation when transfected with FUT1 or FUT2 siRNA (45). We have previously shown that, compared to wild-type mouse lung ECs, FUT2 gene–deficient mouse lung ECs have less chemotactic activity toward basic fibroblast growth factor, and that FUT2 gene–deficient mouse lung ECs have lower fibroblast growth factor receptor 2 expression (46). In this study, we found that mouse lung ECs isolated from FUT1 gene–deficient mice had decreased migration toward VEGF compared to wild-type mouse lung ECs, indicating that FUT1 plays an important role in EC chemotaxis. We also found that FUT1 antisense ODN–transfected HMVEC–conditioned medium had less HMVEC chemotactic activity than FUT1 sense ODN–transfected HMVEC–conditioned medium. This result indicates that FUT1 affects EC migration not only directly but also indirectly, as it appears that angiogenic factors may be secreted from HMVECs, mediated by FUT1 expression.

MCP-1/CCL2 and RANTES/CCL5 are well-known chemokines that induce angiogenesis and leukocyte recruitment (34,40). We found that MCP-1/CCL2 and RANTES/CCL5 secretion was up-regulated in HMVECs by IL-1β. We also found that MCP-1/CCL2 and RANTES/CCL5 levels were decreased in IL-1β–stimulated FUT1 gene–deficient mouse lung EC–conditioned medium compared to similarly treated control–conditioned medium. These findings point to FUT1 as a critical intermediary in expression of some angiogenic chemokines known to be important in RA pathogenesis.

In summary, our study demonstrated that α(1,2)-linked fucosylated proteins are expressed on RA ST endothelial cells, and that α(1,2)-linked fucosylated proteins in RA SF have angiogenic ability. We also found that α(1,2)-linked fucosylated MCP-1/CCL2 was present in RA SF, and that the level of α(1,2)-linked fucosylated MCP-1/CCL2 was significantly elevated in RA SF compared to OA SF. Finally, we showed that blocking FUT1 in ECs reduced CC chemokine production and EC migration. Taken together, these results demonstrate the importance of α(1,2)-linked fucosylation by FUT1 in RA angiogenesis.

ACKNOWLEDGMENTS

We thank the Consortium for Functional Glycomics for providing FUT1 gene–deficient mice. We also thank the personnel at the Cancer Center Immunology Core of University of Michigan for some chemokine ELISAs.

AUTHOR CONTRIBUTIONS

All authors were involved in drafting the article or revising it critically for important intellectual content, and all authors approved the final version to be published. Dr. Isozaki had full access to all of the

data in the study and takes responsibility for the integrity of the data and the accuracy of the data analysis.

Study conception and design. Isozaki, Amin, Ruth, Campbell, Stinson, Koch.

Acquisition of data. Isozaki, Amin, Ruth, Campbell, Tsou, Ha, Domino, Stinson.

Analysis and interpretation of data. Isozaki, Amin, Ruth, Campbell, Koch.

REFERENCES

1. Moremen KW, Tiemeyer M, Nairn AV. Vertebrate protein glycosylation: diversity, synthesis and function. Nat Rev Mol Cell Biol 2012;13:448–62.
2. Moelants EA, Mortier A, Grauwen K, Ronsse I, Van Damme J, Proost P. Citrullination of TNF-α by peptidylarginine deiminases reduces its capacity to stimulate the production of inflammatory chemokines. Cytokine 201;61:161–7.
3. Hart GW. Glycosylation. Curr Opin Cell Biol 1992;4:1017–23.
4. Kannagi R, Izawa M, Koike T, Miyazaki K, Kimura N. Carbohydrate-mediated cell adhesion in cancer metastasis and angiogenesis. Cancer Sci 2004;95:377–84.
5. Miyoshi E, Moriwaki K, Nakagawa T. Biological function of fucosylation in cancer biology. J Biochem 2008;143:725–9.
6. Fukushima K, Satoh T, Baba S, Yamashita K. α1,2-Fucosylated and β-N-acetylgalactosaminylated prostate-specific antigen as an efficient marker of prostatic cancer. Glycobiology 2010;20:452–60.
7. Yoshida M, Takimoto R, Murase K, Sato Y, Hirakawa M, Tamura F, et al. Targeting anticancer drug delivery to pancreatic cancer cells using a fucose-bound nanoparticle approach. PLoS One 2012;7:e39545.
8. Kelly RJ, Rouquier S, Giorgi D, Lennon GG, Lowe JB. Sequence and expression of a candidate for the human Secretor blood group α(1,2)fucosyltransferase gene (FUT2): homozygosity for an enzyme-inactivating nonsense mutation commonly correlates with the non-secretor phenotype. J Biol Chem 1995;270:4640–9.
9. Larsen RD, Ernst LK, Nair RP, Lowe JB. Molecular cloning, sequence, and expression of a human GDP-L-fucose:β-D-galactoside 2-α-L-fucosyltransferase cDNA that can form the H blood group antigen. Proc Natl Acad Sci U S A 1990;87:6674–8.
10. Koch AE, Halloran MM, Haskell CJ, Shah MR, Polverini PJ. Angiogenesis mediated by soluble forms of E-selectin and vascular cell adhesion molecule-1. Nature 1995;376:517–9.
11. Halloran MM, Carley WW, Polverini PJ, Haskell CJ, Phan S, Anderson BJ, et al. Ley/H: an endothelial-selective, cytokine-inducible, angiogenic mediator. J Immunol 2000;164:4868–77.
12. Zhu K, Amin MA, Kim MJ, Katschke KJ Jr, Park CC, Koch AE. A novel function for a glucose analog of blood group H antigen as a mediator of leukocyte-endothelial adhesion via intracellular adhesion molecule 1. J Biol Chem 2003;278:21869–77.
13. Koch AE, Kunkel SL, Burrows JC, Evanoff HL, Haines GK, Pope RM, et al. Synovial tissue macrophage as a source of the chemotactic cytokine IL-8. J Immunol 1991;147:2187–95.
14. Ritchlin C. Fibroblast biology: effector signals released by the synovial fibroblast in arthritis. Arthritis Res 2000;2:356–60.
15. Weinblatt ME, Keystone EC, Furst DE, Moreland LW, Weisman MH, Birbara CA, et al. Adalimumab, a fully human anti–tumor necrosis factor α monoclonal antibody, for the treatment of rheumatoid arthritis in patients taking concomitant methotrexate: the ARMADA trial. Arthritis Rheum 2003;48:35–45.
16. Mori K, Iida S, Yamane-Ohnuki N, Kanda Y, Kuni-Kamochi R, Nakano R, et al. Non-fucosylated therapeutic antibodies: the next generation of therapeutic antibodies. Cytotechnology 2007;55:109–14.
17. Folkman J, Shing Y. Angiogenesis. J Biol Chem 1992;267:10931–4.
18. Carmeliet P. Angiogenesis in life, disease and medicine. Nature 2005;438:932–6.
19. Domino SE, Zhang L, Gillespie PJ, Saunders TL, Lowe JB. Deficiency of reproductive tract α(1,2)fucosylated glycans and normal fertility in mice with targeted deletions of the FUT1 or FUT2 α(1,2)fucosyltransferase locus. Mol Cell Biol 2001;21:8336–45.
20. Domino SE, Zhang L, Lowe JB. Molecular cloning, genomic mapping, and expression of two Secretor blood group α(1,2)fucosyltransferase genes differentially regulated in mouse uterine epithelium and gastrointestinal tract. J Biol Chem 2001;276:23748–56.
21. Iwamori M, Domino SE. Tissue-specific loss of fucosylated glycolipids in mice with targeted deletion of α(1,2)fucosyltransferase genes. Biochem J 2004;380:75–81.
22. Marelli-Berg FM, Peek E, Lidington EA, Stauss HJ, Lechler RI. Isolation of endothelial cells from murine tissue. J Immunol Methods 2000;244:205–15.
23. Ruth JH, Volin MV, Haines GK III, Woodruff DC, Katschke KJ Jr, Woods JM, et al. Fractalkine, a novel chemokine in rheumatoid arthritis and in rat adjuvant-induced arthritis. Arthritis Rheum 2001;44:1568–81.
24. Isozaki T, Rabquer BJ, Ruth JH, Haines GK III, Koch AE. ADAM-10 is overexpressed in rheumatoid arthritis synovial tissue and mediates angiogenesis. Arthritis Rheum 2013;65:98–108.
25. Marotte H, Tsou PS, Rabquer BJ, Pinney AJ, Fedorova T, Lalwani N, et al. Blocking of interferon regulatory factor 1 reduces tumor necrosis factor α–induced interleukin-18 bioactivity in rheumatoid arthritis synovial fibroblasts by induction of interleukin-18 binding protein a: role of the nuclear interferon regulatory factor 1–NF-κB–c-jun complex. Arthritis Rheum 2011;63:3253–62.
26. Rabquer BJ, Pakozdi A, Michel JE, Gujar BS, Haines GK III, Imhof BA, et al. Junctional adhesion molecule C mediates leukocyte adhesion to rheumatoid arthritis synovium. Arthritis Rheum 2008;58:3020–9.
27. Volin MV, Woods JM, Amin MA, Connors MA, Harlow LA, Koch AE. Fractalkine: a novel angiogenic chemokine in rheumatoid arthritis. Am J Pathol 2001;159:1521–30.
28. Park CC, Morel JC, Amin MA, Connors MA, Harlow LA, Koch AE. Evidence of IL-18 as a novel angiogenic mediator. J Immunol 2001;167:1644–53.
29. Amin MA, Volpert OV, Woods JM, Kumar P, Harlow LA, Koch AE. Migration inhibitory factor mediates angiogenesis via mitogen-activated protein kinase and phosphatidylinositol kinase. Circ Res 2003;93:321–9.
30. Marotte H, Ruth JH, Campbell PL, Koch AE, Ahmed S. Green tea extract inhibits chemokine production, but up-regulates chemokine receptor expression, in rheumatoid arthritis synovial fibroblasts and rat adjuvant-induced arthritis. Rheumatology (Oxford) 2010;49:467–79.
31. Macartney JC. Fucose-containing antigens in normal and neoplastic human gastric mucosa: a comparative study using lectin histochemistry and blood group immunohistochemistry. J Pathol 1987;152:23–30.
32. Koch AE, Kunkel SL, Harlow LA, Johnson B, Evanoff HL, Haines GK, et al. Enhanced production of monocyte chemoattractant protein-1 in rheumatoid arthritis. J Clin Invest 1992;90:772–9.
33. Hachicha M, Rathanaswami P, Schall TJ, McColl SR. Production of monocyte chemotactic protein–1 in human type B synoviocytes: synergistic effect of tumor necrosis factor α and interferon-γ. Arthritis Rheum 1993;36:26–34.
34. Volin MV, Shah MR, Tokuhira M, Haines GK, Woods JM, Koch AE. RANTES expression and contribution to monocyte chemotaxis in arthritis. Clin Immunol Immunopathol 1998;89:44–53.
35. Apweiler R, Hermjakob H, Sharon N. On the frequency of protein glycosylation, as deduced from analysis of the SWISS-PROT database. Biochim Biophys Acta 1999;1473:4–8.

36. Hakomori S. Aberrant glycosylation in tumors and tumor-associated carbohydrate antigens. Adv Cancer Res 1989;52:257–331.
37. Nakagawa T, Uozumi N, Nakano M, Mizuno-Horikawa Y, Okuyama N, Taguchi T, et al. Fucosylation of N-glycans regulates the secretion of hepatic glycoproteins into bile ducts. J Biol Chem 2006;281:29797–806.
38. Przybysz M, Maszczak D, Borysewicz K, Szechinski J, Katnik-Prastowska I. Relative sialylation and fucosylation of synovial and plasma fibronectins in relation to the progression and activity of rheumatoid arthritis. Glycoconj J 2007;24:543–50.
39. Ferens-Sieczkowska M, Kossowska B, Gancarz R, Dudzik D, Knas M, Popko J, et al. Fucosylation in synovial fluid as a novel clinical marker for differentiating joint diseases: a preliminary study. Clin Exp Rheumatol 2007;25:92–5.
40. Salcedo R, Ponce ML, Young HA, Wasserman K, Ward JM, Kleinman HK, et al. Human endothelial cells express CCR2 and respond to MCP-1: direct role of MCP-1 in angiogenesis and tumor progression. Blood 2000;96:34–40.
41. Isozaki T, Ruth JH, Amin MA, Campbell PL, Tsou PS, Ha CM, et al. Fucosyltransferase 1 mediates angiogenesis, cell adhesion and rheumatoid arthritis synovial tissue fibroblast proliferation. Arthritis Res Ther 2014;16:R28.
42. Proost P, Struyf S, Couvreur M, Lenaerts JP, Conings R, Menten P, et al. Posttranslational modifications affect the activity of the human monocyte chemotactic proteins MCP-1 and MCP-2: identification of MCP-2(6-76) as a natural chemokine inhibitor. J Immunol 1998;160:4034–41.
43. Carlyon JA, Akkoyunlu M, Xia L, Yago T, Wang T, Cummings RD, et al. Murine neutrophils require α1,3-fucosylation but not PSGL-1 for productive infection with Anaplasma phagocytophilum. Blood 2003;102:3387–95.
44. Mathieu S, Gerolami R, Luis J, Carmona S, Kol O, Crescence L, et al. Introducing α(1,2)-linked fucose into hepatocarcinoma cells inhibits vasculogenesis and tumor growth. Int J Cancer 2007;121:1680–9.
45. Palumberi D, Aldi S, Ermini L, Ziche M, Finetti F, Donnini S, et al. RNA-mediated gene silencing of FUT1 and FUT2 influences expression and activities of bovine and human fucosylated nucleolin and inhibits cell adhesion and proliferation. J Cell Biochem 2010;111:229–38.
46. Tsou PS, Ruth JH, Campbell PL, Isozaki T, Lee S, Marotte H, et al. A novel role for inducible Fut2 in angiogenesis. Angiogenesis 2013;16:195–205.